COMSOL
CONFERENCE
2024 BOSTON

Potential Fields Modeling to Support Machine Learning Applications in Maritime Environments

J. McKenna[1], J. Karst[2], J. Luttrell IV[1], R. Riedel[1], S. Kar[3], and P. Duff[4]
1. Roger F. Wicker Center for Ocean Enterprise, The University of Southern Mississippi Gulfport, MS, USA
2. CTI, Columbus, OH, USA
3. RENCI, Chapel Hill, NC, USA
4. Naval Research Laboratory, Bay St. Louis, MS, USA

Abstract
The integration of machine learning (ML) techniques into geophysical exploration and underwater mapping has emerged as a transformative approach for interpreting complex sensor data. This paper presents a comprehensive framework for using COMSOL Multiphysics to develop and validate potential field models—specifically gravity and magnetics—in maritime environments. These models are designed to support machine learning applications, particularly for enhancing the predictive capabilities of uncrewed underwater vehicles (UUVs). In the maritime context, accurate modeling of gravity and magnetic fields is crucial for detecting and characterizing underwater objects, ranging from low to high magnetic targets such as unexploded ordnance (UXO), shipwrecks, and geological features. We have developed a sandbox environment using COMSOL Multiphysics that allows for the precise creation and manipulation of complex geophysical sensing. This environment enables the detailed simulation of potential fields incorporating various target properties and environmental conditions to generate synthetic datasets for ML training.

Keywords: UXO, Geophysics, Machine Learning, CNN, LSTM, Magnetostatics, Magnetic Anomaly, USV.

Introduction
Measurements of magnetic anomalies caused by ferromagnetic objects is a widely used technique [1], especially with the rapid advancement of geomagnetic technologies [2], [3]. In the maritime context, accurate modeling of potential (gravity and magnetic) fields is important for detecting and characterizing underwater objects [4], [5], [6], [7], ranging from low to high magnetic targets, such as unexploded ordnance (UXO), shipwrecks, and geological features [8], [9], [10], [11].

Because of the constant change in Earth's magnetic field, it is difficult to make predictions of field states into the distant future based on observations alone. Additionally, much of the surface of the earth is not magnetically mapped at a fine enough resolution for anomaly detection. Adequate measurement of needed data may not be possible[12], calling on simulation methods to fill the data gap. Magnetic field modeling may be taken as a complementary approach to methods relying on field data collection. Moreover, simulation for training machine learning (ML) models offers more robust methods to detect, classify, and even localize the source of magnetic anomalies [14], [15].

We have developed a framework for magnetic field modeling using high resolution vector data from magnetic sensors. The framework is based on a sandbox environment using COMSOL Multiphysics that allows for the precise creation and manipulation of complex geophysical targets and observation platforms. Our environment enables the detailed simulation of potential fields incorporating various target properties and environmental conditions to generate synthetic datasets for subsequent algorithm development using ML approaches.

Experimental Set Up
Our simulation model started with the definition of target object physical properties and the spatial configuration. Low, medium, and high magnetic targets were systematically introduced into the simulation space, and their interactions with the surrounding medium calculated. The gravity and magnetic anomalies generated by these targets were subsequently recorded from various UUV simulations, providing a rich dataset capturing the nuances of potential field variations in different scenarios.

To validate our models, we employed a combination of theoretical predictions and empirical data. The theoretical framework was couched in well-established geophysical principles, ensuring alignment between synthetic data and expected physical behaviors.

Empirical validation was conducted using field measurements from controlled maritime environments where known targets were surveyed with high-precision gravity and magnetic sensors. Experiments for empirical validation were

conducted by drawing a sensor platform between two points across the water's surface, about 70 meters using a winch system to keep the sensor platform well constrained to its linear path. This process was repeated for several trials per target, and for several target types and depths. Data was logged by various sensors including Magnetic, IMU, and GPS enhanced with RTK (Figure 1a). The minimization between the simulated B field and empirical data is the metric we hope to minimize (Figure 1b).

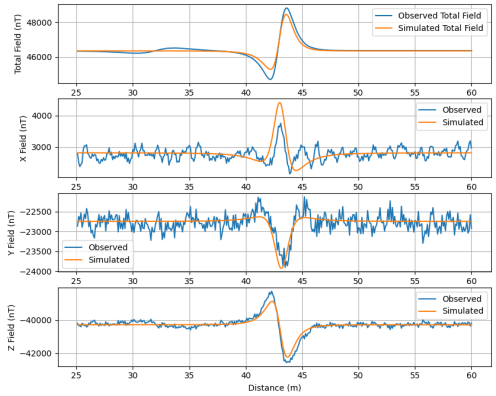

Figure 1. (a) Low magnetic test platform hosting the sensor array. The platform travels along a tension line under which magnetic targets are placed. (b) Optimized analytic modeling of observed data.

Methods

For our modeling process, we used the M*agnetic Fields, No Currents* interface in COMSOL 6.2, allowing the Poisson equation for magnetostatics: $-\nabla \cdot (\mu_0 \nabla V_m - \mu_0 M_0) = 0$ to more easily be incorporated into simulation runs. Figure 2 shows the modeled isopipe targets which are thin, hollow cylinders of 12 in or 24 in length. Model parameters are given in Table 1.

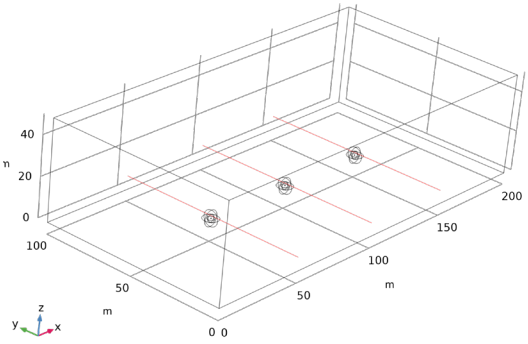

Figure 2. Hollow isopipe metallic targets. Targets are (from left to right) orthogonal, vertical, and parallel to the cut lines shown.

Table 1: ***COMSOL Model Parameters***

mur_pipe	50 or 100 or 200	Relative permeability
H0	46353.6[nT]	Local geomagnetic field
Incl	58.77291[deg]	Local inclination
Decl	-4.28[deg]	Local Declination
xx	12 or 24[in]	Length of pipe
pir	4.026[in]	Pipe inner radius
por	4.5[in]	Pipe outer radius

COMSOL Simulations

Figure 3 a-d shows sample total magnetic field (i.e. the scalar field) as well as the vector components of the modeled B field as a sensor array moves 1m over a series of 12 in pipe targets along the cut lines shown in Figure 2.

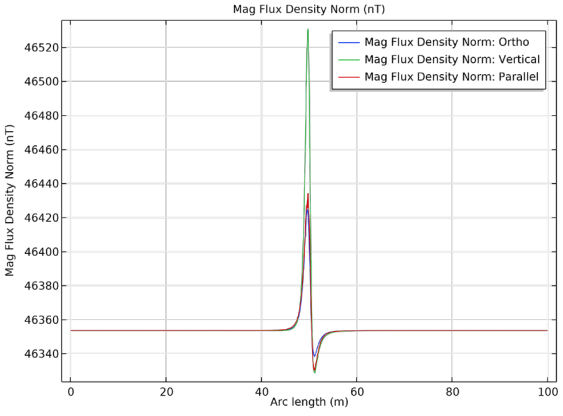

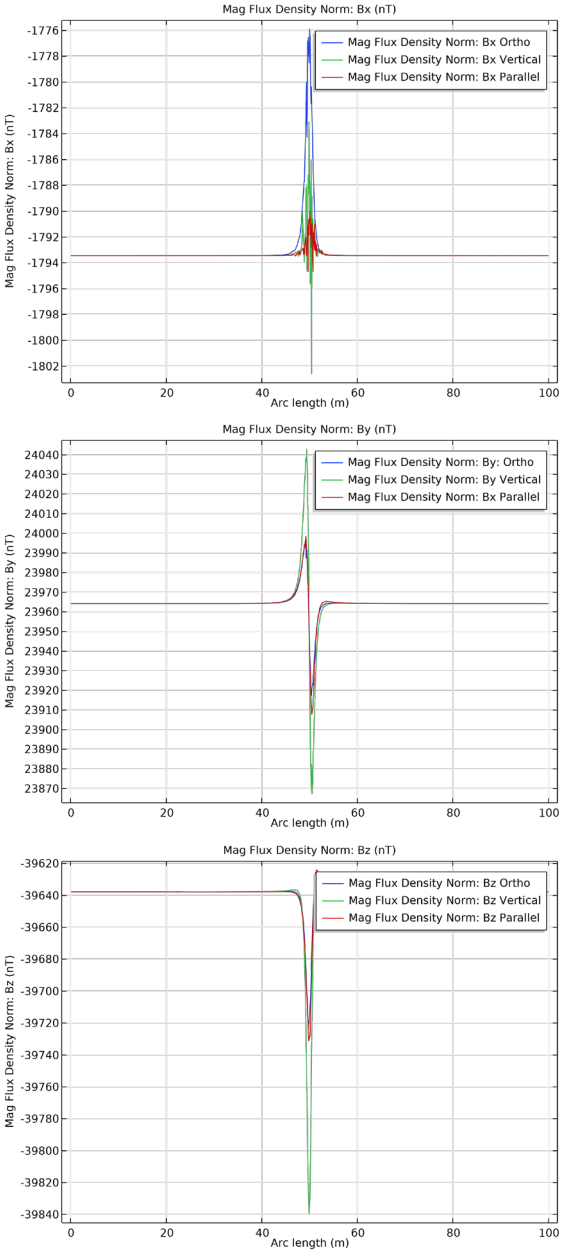

Figure 3a-d. Simulated magnetic anomalies over a 12 in pipe target at various orientations. From top to bottom: Total B field, Bx, By, and Bz. Bx is not as accurate due to the model geometry. In both cases the relative permeability was 100.

As the sensor array moves up to 5m above the targets, the magnetic anomalies observed decrease significantly as expected. This is shown in Figure 4, where the total modeled B field is shown for a sensor array 1m and 5m above 24 in targets. We observed the modeled data drops from ~1,000nT to ~100 nT.

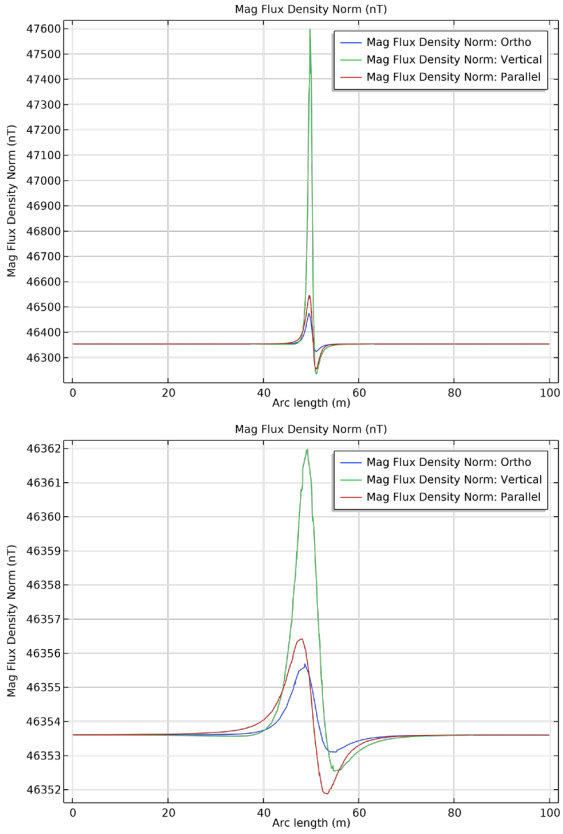

Figure 4a-b. Total B field over 24 in targets. The height of the sensor array is 1m (top), and 5m above the target (bottom). In both cases the relative permeability was 200.

The COMSOL models accurately reproduced static magnetic anomaly data due to the interaction of the local geomagnetic field with ferrous targets of various sizes and geometries. These models included material polarization due to the inducing field and self-demagnetization effects.

Machine Learning Models

We now use Machine Learning (ML) techniques on data generated by our COMSOL simulation models. Due to the sequential nature of the simulated data and because simulations generated continuous observations, the machine learning approach included Long Short-Term Memory (LSTM) network, regression, tree boosting, and Deep Neural Network (DNN) models. The LSTM model was for assessing prediction performance when running on simulated sensor sequence data, thus estimating the effectiveness of using simulated data as a data augmentation process for potentially supplementing observational data. The other ML models were chosen for confirmation of simulation data patterns. For the Boosting technique, sensor readings were dichotomized to produce a label reflecting above and below the unsigned reading mean. For predictors, target permeability, target aspect ratio, and the speed of the UUV were used for training the boosting ML model.

Models were run on simulated data only. LSTM models were run using an embedding sequence of 10 data points from a total of over 500,000. Confirmatory ML models were run using a 1m, 3m, and 5m simulated vertical distance between the sensor and target. A regression model and a DNN model were trained using the simulated vector components of the B field as predictors. The DNN model architecture comprised a flattened input layer, two fully connected layers with 20 nodes each, a dropout layer set to 0.5 after each fully connected layer, and an output softmax layer. The DNN model was run using the ReLU activation function, the Adam optimizer, a batch size of 50, a dropout rate of 0.14, and a learning rate of 0.0001. The regression model was constructed to test how effectively data sensor total field from simulation of a 12 in diameter target predicted the simulated total field data from a 24 in diameter target. The DNN model was trained for 1,000 epochs.

The models above served as the foundation for training advanced ML algorithms, with a particular focus on sequence data. ML models are well-suited for sequence data [16], [17], [18], such as time-series analysis, making them ideal for interpreting UUV integrated sensor data as they navigate underwater. The synthetic datasets generated from our COMSOL models provide diverse training examples, allowing ML models to learn the complex temporal relationships and signature patterns associated with different target types.

Each ML model was assessed for its ability to accurately classify and predict sensor signatures under two sensor-to-target distances. By leveraging the robustness and versatility of COMSOL Multiphysics in combination with cutting-edge ML techniques, we aim to develop predictive models that significantly enhance the detection and characterization capabilities of UUVs.

Machine Learning Regression Model Governing Equations

Of the ML methods used, only regression may be best represented by a closed-form equation. The LSTM and DNN techniques were based on architectures. The equation for the ML regression model was

$$y = \beta_0+\beta_1X_1+\beta_2X_2+\ldots+\beta_nX_n+e, \text{ where}$$

y is the dependent variable, β_0 is the intercept, β are coefficients, X are the predictors, and e is the independent and identically distributed error term.

Results and Discussion

Modeling findings indicated a close agreement between simulated and observed total field data, with vector data showing higher noise levels (Figure 2). Measured magnetic field vector data is commonly of higher noise due to hardware limitations, whereas total field is measured separately, lowering signal noise.

The LSTM model showed promising findings for using simulation as a data augmentation approach for supplementing observational data (Figure 5). Less so for Y-field predictions, large dipole peak predictions were of lower agreement between simulated and LSTM data. When training a regression model on simulated data (Figure 6), an R^2 of over 0.98 was estimated. Performance for the DNN was also promising (Figure 7), but it may require more training data and future work to extend findings to other sensor data. The regression model was trained with strong regularization to foster generalizability and was still able to achieve a good fit. Conversely, the boosting model did not show strong predictor effects, as the accuracy was only around 0.5. Permeability was the feature of highest importance (0.44) in determining model accuracy. Target aspect ratio (0.30) and UUV speed (0.26) were of similar importance.

Of note, the poor results of the boosting algorithm may be associated with the low contrast among sensor signal differences from predictors. Permeability being the most important predictor makes sense, due to the different influence on magnetic fields from object density [19]. Perhaps an increase in sample size might unveil small-scale differences in signals due to target shape or sensor movement speed.

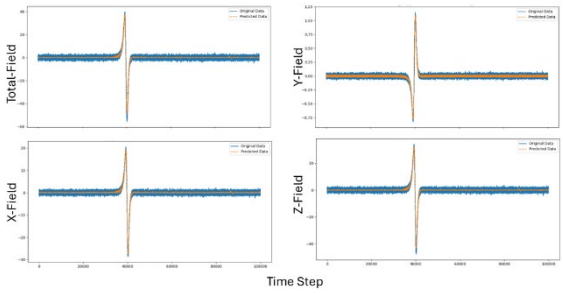

Figure 5. LSTM model fit to simulated sensor data; peaks are dipoles.

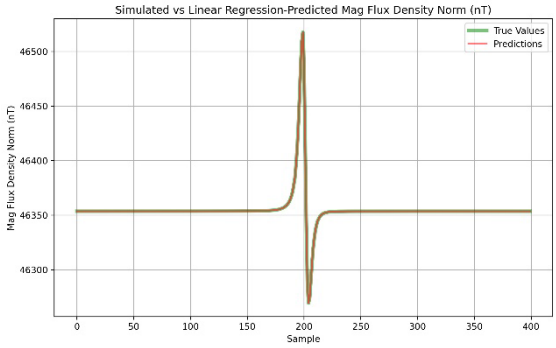

Figure 6. Sensor data prediction performance of a regression model fit to simulated 12 in pipe target data and tested on simulated 24 in pipe target data (relative permeability was set to 50 for both targets).

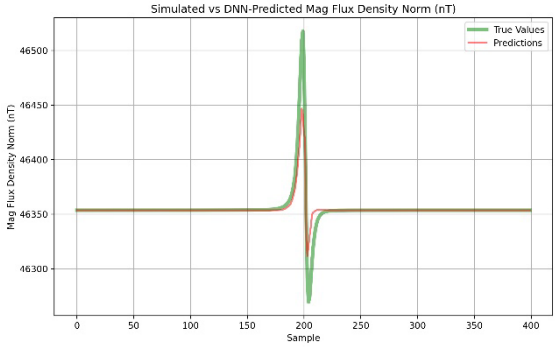

Figure 7. Sensor data prediction performance of a DNN model trained on simulated 12 in pipe target data and tested on simulated 24 in pipe target data (relative permeability was set to 50 for both targets).

Conclusions

Our approach demonstrates the critical role of validated potential fields modeling in supporting ML applications. The sandbox environment not only facilitates the generation of high-fidelity training data but also provides a controlled setting for testing and refining ML algorithms before deployment in real-world scenarios. The implications of this work extend beyond underwater exploration, offering a blueprint for integrating simulation-driven ML in various geophysical and engineering domains.

As this work points toward the successful integration of simulation and ML approaches, future work to advance the benefits from this study needs to be highlighted. A potentially fruitful undertaking may be to test observational data as a check for ML models based on simulations, especially in areas where observation data are not size-limited. Comparing ML models trained on simulations and tested on observations (or vice-versa) may, with repetition and time, point toward better parameterization of both simulated and ML models as causes for ML performance limitations can be unveiled.

Additional future work may be conducted to allow more readily deployable ML models for field operations. Generating prediction ML models to estimate distance to target and target type are essential for field operations, especially for cleanups in post-war dumping and military test areas [4], [20], [21]. Another area of work to extend the benefits of this study are edge computing of sensor data [22]. As ML models will be deployed on the edge, offloading computation associated with ML models needs to be carefully planned with limited compute resources in mind, such as simpler ML model architectures. This study would be remiss if it did not mention sensor data pipelines. Sensor data is commonly of large volume and velocity, requiring careful implementation planning for its transfer and storage. Data storage is imperative for the continuous training and testing of ML models, including assessing the effectiveness of deployed models.

In closing, the fusion of COMSOL Multiphysics modeling with machine learning represents a powerful synergy, enabling the development of intelligent UUV systems capable of autonomously interpreting complex geophysical data. This research underscores the potential of advanced modeling and ML to drive innovation in maritime surveillance and beyond.

References

[1] Y. Zhao *et al.*, “A brief review of magnetic anomaly detection,” *Meas. Sci. Technol.*, vol. 32, no. 4, p. 042002, Feb. 2021, doi: 10.1088/1361-6501/abd055.

[2] J. Zhang, X. Xiang, and W. Li, “Advances in Marine Intelligent Electromagnetic Detection System, Technology, and Applications: A Review,” *IEEE Sensors Journal*, vol. 23, no. 5, pp. 4312–4326, Mar. 2023, doi: 10.1109/JSEN.2021.3129286.

[3] M. A. Khan, J. Sun, B. Li, A. Przybysz, and J. Kosel, “Magnetic sensors-A review and recent technologies,” *Eng. Res. Express*, vol. 3, no. 2, p. 022005, Jun. 2021, doi: 10.1088/2631-8695/ac0838.

[4] Z. Wen, S. Han, C. Gao, Y. Chen, L. Guo, and Y. Zhang, “A Deep Learning Method for Recognizing Types of Unexploded Ordnance Based on Magnetic Detection,” *IEEE Transactions on Geoscience and Remote Sensing*, vol. 62, pp. 1–13, 2024, doi: 10.1109/TGRS.2024.3405478.

[5] J. Tang, S. Hu, Z. Ren, and C. Chen, “Localization of Multiple Underwater Objects With Gravity Field and Gravity Gradient Tensor,” *IEEE Geoscience and Remote Sensing Letters*, vol. 15, no. 2, pp. 247–251, Feb. 2018, doi: 10.1109/LGRS.2017.2784837.

[6] S. Hu *et al.*, “Multiple Underwater Objects Localization With Magnetic Gradiometry,”

IEEE Geoscience and Remote Sensing Letters, vol. 16, no. 2, pp. 296–300, Feb. 2019, doi: 10.1109/LGRS.2018.2870839.

[7] F. Zeng, X. Zhang, J. Liu, H. Li, Z. Zhu, and S. Zhang, "Magnetic Gradient Tensor Positioning Method Implemented on an Autonomous Underwater Vehicle Platform," *Journal of Marine Science and Engineering*, vol. 11, no. 10, Art. no. 10, Oct. 2023, doi: 10.3390/jmse11101909.

[8] G. Loureiro, A. Dias, J. Almeida, A. Martins, S. Hong, and E. Silva, "A Survey of Seafloor Characterization and Mapping Techniques," *Remote Sensing*, vol. 16, no. 7, Art. no. 7, Jan. 2024, doi: 10.3390/rs16071163.

[9] M. Pilkington, A. R. Hildebrand, and C. Ortiz-Aleman, "Gravity and magnetic field modeling and structure of the Chicxulub Crater, Mexico," *Journal of Geophysical Research: Planets*, vol. 99, no. E6, pp. 13147–13162, 1994, doi: 10.1029/94JE01089.

[10] D. Cristaudo, B. M. Gross, and J. A. Puleo, "Momentum Balance Analysis of Spherical Objects and Long-Term Field Observations of Unexploded Ordnance (UXO) in the Swash Zone," *Journal of Marine Science and Engineering*, vol. 11, no. 1, Art. no. 1, Jan. 2023, doi: 10.3390/jmse11010079.

[11] M. Blachnik, R. Przyłucki, S. Golak, P. Ściegienka, and T. Wieczorek, "On the Development of a Digital Twin for Underwater UXO Detection Using Magnetometer-Based Data in Application for the Training Set Generation for Machine Learning Models," *Sensors*, vol. 23, no. 15, Art. no. 15, Jan. 2023, doi: 10.3390/s23156806.

[12] X. Sun, Y. Liu, J. T. Hoeksema, K. Hayashi, and X. Zhao, "A New Method for Polar Field Interpolation," *Sol Phys*, vol. 270, no. 1, pp. 9–22, May 2011, doi: 10.1007/s11207-011-9751-4.doi: 10.1007/s11214-023-00983-x.

[13]N. F. Putman, "Animal Navigation: Seabirds Home to a Moving Magnetic Target," *Current Biology*, vol. 30, no. 14, pp. R802–R804, Jul. 2020, doi: 10.1016/j.cub.2020.05.061.

[14]S. Pollok, N. Olden-Jørgensen, P. S. Jørgensen, and R. Bjørk, "Magnetic field prediction using generative adversarial networks," *Journal of Magnetism and Magnetic Materials*, vol. 571, p. 170556, Apr. 2023, doi: 10.1016/j.jmmm.2023.170556.

[15]D. Telloni *et al.*, "Prediction Capability of Geomagnetic Events from Solar Wind Data Using Neural Networks," *ApJ*, vol. 952, no. 2, p. 111, Jul. 2023, doi: 10.3847/1538-4357/acdeea.

[16]E. A. Belalcazar-Bolaños, D. Torricelli, and J. L. Pons, "Automatic Detection of Magnetic Disturbances in Magnetic Inertial Measurement Unit Sensors Based on Recurrent Neural Networks," *Sensors*, vol. 23, no. 24, Art. no. 24, Jan. 2023, doi: 10.3390/s23249683.

[17]A. Collado-Villaverde, P. Muñoz, and C. Cid, "Deep Neural Networks With Convolutional and LSTM Layers for SYM-H and ASY-H Forecasting," *Space Weather*, vol. 19, no. 6, p. e2021SW002748, 2021, doi: 10.1029/2021SW002748.

[18]X. Wu, S. Huang, M. Li, and Y. Deng, "Vector Magnetic Anomaly Detection via an Attention Mechanism Deep-Learning Model," *Applied Sciences*, vol. 11, no. 23, Art. no. 23, Jan. 2021, doi: 10.3390/app112311533.

[19]Z. Deng, Y. Sun, Y. Kang, K. Song, and R. Wang, "A Permeability-Measuring Magnetic Flux Leakage Method for Inner Surface Crack in Thick-Walled Steel Pipe," *J Nondestruct Eval*, vol. 36, no. 4, p. 68, Sep. 2017, doi: 10.1007/s10921-017-0447-z.

[20]M. Seidel, T. Frey, and J. Greinert, "Underwater UXO detection using magnetometry on hovering AUVs," *Journal of Field Robotics*, vol. 40, no. 4, pp. 848–861, 2023, doi: 10.1002/rob.22159.

[21]M. D. Wigh, M. E. Kolster, T. M. Hansen, and A. Døssing, "Classification of UXO and non-UXO from magnetic anomaly data: a case study on inversion of drone magnetic data from Rømø, Denmark," *Geophysical Journal International*, vol. 234, no. 2, pp. 915–932, Aug. 2023, doi: 10.1093/gji/ggad097.

[22]S. Lu, J. Lu, K. An, X. Wang, and Q. He, "Edge Computing on IoT for Machine Signal Processing and Fault Diagnosis: A Review," *IEEE Internet of Things Journal*, vol. 10, no. 13, pp. 11093–11116, Jul. 2023, doi: 10.1109/JIOT.2023.3239944.

Acknowledgements

We thank Chuck Key, Megan McKenzie, William Rippy, James Thompson, and Alison Kinnaman for collecting the field data.